Novel structures and electromagnetic properties of the A-site-ordered/disordered manganites $RBaMn_2O_6/R_{0.5}Ba_{0.5}MnO_3$ (R = Y and rare earth elements)

2004 J. Phys.: Condens. Matter 16 S573

(http://iopscience.iop.org/0953-8984/16/11/002)

INSTITUTE OF PHYSICS PUBLISHING JOURNAL OF PHYSICS: CONDENSED MATTER

J. Phys.: Condens. Matter **16** (2004) S573–S583 PII: S0953-8984(04)74075-8

Novel structures and electromagnetic properties of the A-site-ordered/disordered manganites $RBaMn_2O_6/R_{0.5}Ba_{0.5}MnO_3$ (R = Y and rare earth elements)

Yutaka Ueda and Tomohiko Nakajima

Materials Design and Characterization Laboratory, Institute for Solid State Physics, University of Tokyo, 5-1-5 Kashiwanoha, Kashiwa, Chiba 277-8581, Japan

E-mail: yueda@issp.u-tokyo.ac.jp

Received 7 January 2004
Published 4 March 2004
Online at stacks.iop.org/JPhysCM/16/S573 (DOI: 10.1088/0953-8984/16/11/002)

Abstract

The A-site-ordered/disordered manganese perovskites, $RBaMn_2O_6/R_{0.5}Ba_{0.5}MnO_3$ (R = Y and rare earth elements), are reviewed. $RBaMn_2O_6$ displays remarkable features: (1) the charge/orbital order (CO) transition at relatively high temperatures far above 300 K, (2) a new stacking variation of the CE-type CO with a fourfold periodicity along the *c*-axis, (3) the presence of structural transition possibly accompanied by $d_{x^2-y^2}$ orbital order and (4) electronic phase segregation. These novel structural and electromagnetic properties are discussed in terms of the structural characteristic that the MnO_2 square sublattice is sandwiched by two types of rock-salt layer, RO and BaO, with different lattice sizes. Such structure introduces a strong frustration to the MnO_2 sublattice and gives a new perturbation to the competition of multiple degrees of freedom among charge, orbital, spin and lattice. In $R_{0.5}Ba_{0.5}MnO_3$ with a primitive cubic perovskite cell, on the other hand, the magnetic glassy states are dominant as the ground state. A peculiar behaviour, steplike ultrasharp magnetization and resistivity changes, has been observed in $Pr_{0.5}Ba_{0.5}MnO_3$.

1. Introduction

The magnetic and electrical properties of perovskite manganites with the general formula $(R^{3+}_{1-x}A^{2+}_x)MnO_3$ (R = rare earth elements; A = Sr, Ca) have been extensively investigated for the last decade [1]. Among the interesting features are the so-called colossal magnetoresistance (CMR) and metal–insulator (MI) transition accompanied by the charge and orbital order (CO). It is now widely accepted that these interesting phenomena are caused by the strong correlation/competition of multiple degrees of freedom, that is, spin, charge, orbital and lattice.

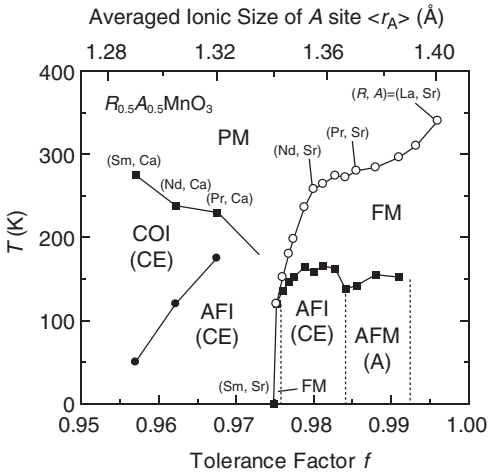

Figure 1. Generalized phase diagram for $(R^{3+}_{0.5}A^{2+}_{0.5})MnO_3$ [1]. FM, ferromagnetic metal; AFM(A), A-type antiferromagnetic metal; COI(CE), CE-type charge/orbital-ordered insulator; AFI(CE), antiferromagnetic CE-type charge/orbital-ordered insulator; PM (or PI), paramagnetic metal (or paramagnetic insulator).

The structure of perovskite $RMnO_3$ consists of an MnO_2 square sublattice and an RO rock-salt sublattice. The mismatch between the larger MnO_2 and the smaller RO sublattices is relaxed by tilting MnO_6 octahedra, leading to lattice distortion from a cubic structure to, mostly, an orthorhombic $GdFeO_3$-type structure with a cell of $\sqrt{2}a_p \times \sqrt{2}b_p \times 2c_p$, where a_p, b_p and c_p denote the primitive cell for the simple cubic perovskite. In this lattice distortion, the bond angle ∠Mn–O–Mn deviates from 180°, resulting in a significant change in the effective one-electron bandwidth (W) or equivalently e_g-electron transfer interaction (t). In the substitution system of $(R^{3+}_{1-x}A^{2+}_x)MnO_3$, not only the doping level but also the bandwidth can be controlled by the substitution of A^{2+} for R^{3+}. In $(R^{3+}_{1-x}A^{2+}_x)MnO_3$ with a fixed x and a random distribution of R^{3+} and A^{2+}, the structural and electromagnetic properties have been explained well by the degree of mismatch, that is, the tolerance factor $f = (\langle r_A\rangle + r_O)/[\sqrt{2}(r_{Mn} + r_O)]$, where $\langle r_A\rangle$, r_{Mn} and r_O are (averaged) ionic radii for the respective elements, because W or t is changed by varying f. Figure 1 shows the generalized phase diagram for $(R_{0.5}A_{0.5})MnO_3$ with the half-doped level ($x = 1/2$; $Mn^{3+}/Mn^{4+} = 1$) [1], where the ferromagnetic metal (FM) generated by the double-exchange (DE) interaction is dominant near $f = 1$ (maximal W or t), while the CE-type charge/orbital-ordered insulator (COI(CE)) is most stabilized in the lower f region ($f < 0.975$). In the middle region ($f \sim 0.975$), the competition between the ferromagnetic DE and antiferromagnetic CO interactions results in various phenomena including the FM to antiferromagnetic charge/orbital-ordered insulator (AFI(CE)) transition or CMR.

Recently, it has been argued that the A-site randomness affects the physical properties of $(R^{3+}_{1-x}A^{2+}_x)MnO_3$. Phenomena such as CMR and electronic phase separation [2] may be induced by the A-site randomness. Although the search for a compound without A-site randomness has been motivated by its intriguing properties, almost all the works devoted to a series of perovskite manganites so far are on the disordered manganites with R^{3+} and A^{2+} ions being randomly distributed. This means that, whenever x is finite, there inevitably exists a disorder in the lattice. Since the physical properties of the perovskite manganite are quite sensitive to even a tiny change in lattice distortion, it is important to employ a compound

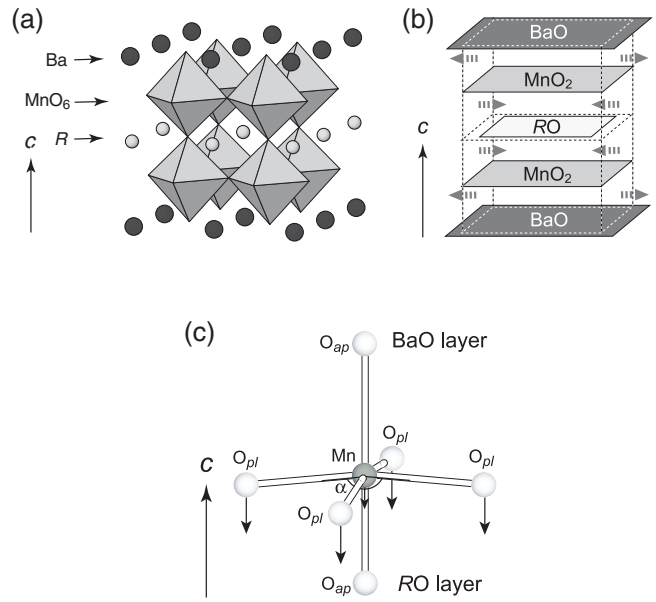

Figure 2. Crystal structure (a) and structural concept (b) of the A-site-ordered manganite $RBaMn_2O_6$, and an illustration of the distorted MnO_6 octahedron (c).

without A-site disorder in order to make clear the effect of A-site randomness. Very recently we successfully synthesized the A-site-ordered manganite, $RBaMn_2O_6$ (R = Y and rare earth elements), and reported its structures and electromagnetic properties [3–7].

The discovery of novel structural and physical properties in the A-site-ordered manganite, $RBaMn_2O_6$, has demanded new comprehension about perovskite manganese oxides [3–11]. It should be emphasized that the A-site-ordered manganite $RBaMn_2O_6$ has a remarkable structural feature in addition to the absence of the A-site randomness. The most significant structural feature of $RBaMn_2O_6$ is that the MnO_2 square sublattice is sandwiched by two types of rock-salt layer, RO and BaO with different lattice sizes, as schematically shown in figure 2. This means that the structural and physical properties of $RBaMn_2O_6$ can no longer be explained in terms of the basic structural distortion, that is f, as in $R_{0.5}A_{0.5}MnO_3$. The lattice size of the AO layer is much smaller in the RO layer and much larger in the BaO layer than that of the MnO_2 layer. The large mismatch between RO and BaO lattices introduces a strong frustration to the MnO_2 sublattice and as a result the MnO_6 octahedron itself is heavily distorted in the way illustrated in figure 2(c). Such deformation must give a new perturbation to the competition of multiple degrees of freedom among charge, orbital, spin and lattice.

In this paper, the structures and electromagnetic properties of the A-site-ordered manganite, $RBaMn_2O_6$, are reviewed and discussed in terms of the structural frustration. Furthermore the structures and electromagnetic properties of the A-site-disordered manganite, $R_{0.5}Ba_{0.5}MnO_3$, are also reported in comparison with the ordered form $RBaMn_2O_6$.

2. Sample preparation and experimental procedures

The synthesis of the A-site-ordered form $RBaMn_2O_6$ requires two procedures. The flowchart is shown in figure 3. Starting reagents R_2O_3, MnO_2 and $BaCO_3$ with 99.99% purities were

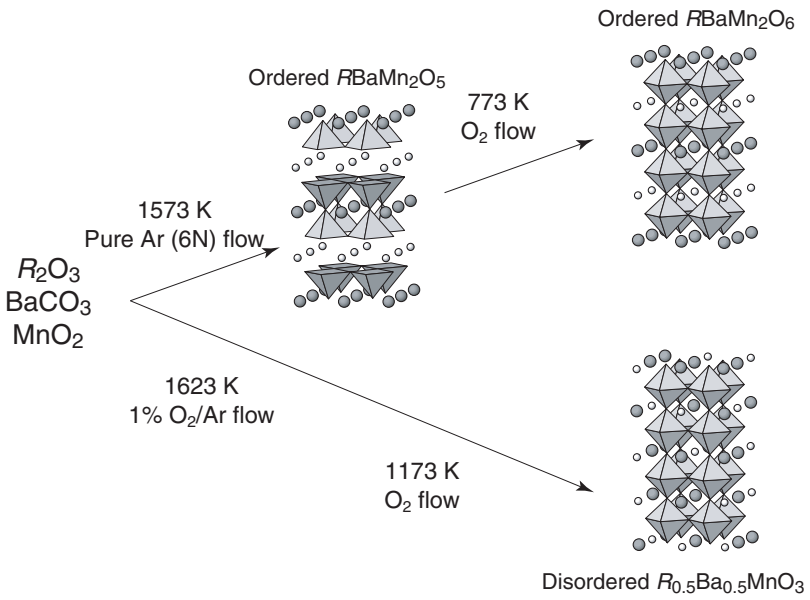

Figure 3. Flowchart of sample preparation.

ground thoroughly, pressed into pellets and calcined in an Ar flow (6 N) at 1573 K for 48 h. This rather reductive atmosphere (6 N Ar; $P_{O_2} < 10^{-4}$ atm) produced oxygen-deficient perovskite, $RBaMn_2O_{6-y}$ ($y \sim 1$), with a layer type ordering of R and Ba and the lack of oxygen in the RO layers. This is due to the general preference of the small R^{3+} ions to take eightfold coordination as realized in $RBaMn_2O_{6-y}$ ($y \sim 1$). Namely, the use of Ar gas is to avoid the formation of the A-site disorder, resulting in $R_{0.5}Ba_{0.5}MnO_3$, in which R^{3+} ions have 12-fold coordination. A similar trend has often been seen in the Ba-based perovskites such as $LaBa_2Cu_3O_7$ and $YBaCo_2O_{5+x}$ [12, 13]. The second step is annealing the obtained specimen in flowing O_2 at 773 K for 48 h, which leads to the full oxidation ($y = 0$) of the specimen without any diffusion of the A-site cations. This reaction is reversible and indicates the topotactic nature of the transformation between $RBaMn_2O_5$ and $RBaMn_2O_6$. Powder samples of the A-site-disordered form $R_{0.5}Ba_{0.5}MnO_3$ were obtained by a solid state reaction of the same starting compounds at 1623 K in 1% O_2/Ar gas, followed by annealing at 1173 K in O_2 gas for 1 day. Annealing of $RBaMn_2O_6$ under O_2 gas at high temperatures gave insufficient R/Ba solid solution.

The obtained products were checked to be of single phase by x-ray diffraction. The order/disorder of R and Ba was carefully checked by the presence/absence of the (001/2) reflection indexed in the primitive cell. The crystal structures were refined by the Rietveld analysis of powder neutron diffraction using RIETAN 2000. Independent refinement of the fractional occupancies of the Ba and R sites in the ordered form showed no antisite disorder to an experimental uncertainty of $\pm 3\%$. The magnetic ordered states at low temperatures were also studied by powder neutron diffraction. The microscopic structures were probed by means of transmission electron microscopy (TEM). The magnetic properties were studied using a SQUID magnetometer in a temperature range $T = 2$–400 K. The electric resistivity of a sintered pellet was measured for $T = 2$–400 K by a conventional four-probe technique.

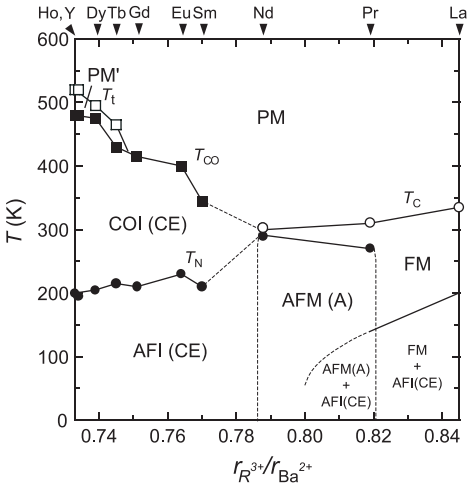

Figure 4. Phase diagram for $RBaMn_2O_6$. The notation for each phase and transition temperature is the same as defined in figure 1 (see text).

3. Structures and electromagnetic properties

3.1. The A-site-ordered manganite, $RBaMn_2O_6$

The crystal structure of $RBaMn_2O_6$ at room temperature has a tetragonal $a_p \times a_p \times 2c_p$ cell with no tilt of MnO_6 octahedra for R = La, Pr and Nd, while it has a larger cell of $\sqrt{2}a_p \times \sqrt{2}b_p \times 2c_p$ with a tilt of MnO_6 octahedra for R = Sm–Y, where a_p and c_p denote the primitive cell for the simple cubic perovskite [4, 7, 8]. The $\sqrt{2}a_p \times \sqrt{2}b_p \times 2c_p$ unit cells for R = Sm, Eu and Gd are tetragonal ($a_p = b_p$) but those for R = Tb, Dy, Ho and Y are distorted to monoclinic [3, 4, 6, 9, 10]. The TEM study reveals an in-plane superstructure of $2\sqrt{2}a_p \times \sqrt{2}b_p$ characteristic of the CE-type CO and a new stacking variation with a fourfold periodicity ($\alpha\alpha\beta\beta$-stacking) along the c-axis for R = Sm–Y [4, 5, 10].

The results of structures and electromagnetic properties for $RBaMn_2O_6$ are summarized in figure 4 in a phase diagram [4]. Here we express the phase diagram as a function of the ratio of ionic radius, $r_I = r_{R^{3+}}/r_{Ba^{2+}}$, instead of f. r_I is a measure of the mismatch between the RO and BaO lattices. $RBaMn_2O_6$ can be classified into three groups from the obtained structural and electromagnetic properties. The first group (R = La, Pr and Nd) has an FM transition at T_C. In $PrBaMn_2O_6$ and $NdBaMn_2O_6$, the FM transition is followed by an A-type antiferromagnetic metal (AFM(A)) transition. A part of the FM phase transforms to AFI(CE) phase in $LaBaMn_2O_6$ and the AFI(CE) phase coexists with the FM phase as the ground state [7]. In $PrBaMn_2O_6$, a small amount of AFI(CE) phase coexists with the AFM(A) phase, while no trace of AFI(CE) is seen in $NdBaMn_2O_6$ [7]. The second group (R = Sm, Eu and Gd) shows an MI transition (paramagnetic metal (PM) to COI(CE) transition) at T_{CO}, and then the COI(CE) phase orders antiferromagnetically at T_N (AFI(CE)). The third group (R = Tb, Dy, Ho and Y) shows the successive three transitions, the structural transition at T_t, CO transition (COI(CE)) at T_{CO} and antiferromagnetic transition (AFI(CE)) at T_N on cooling [3–6]. The structural transition at T_t is not accompanied by either charge or magnetic order. The AFI(CE) phase for R = Sm–Y has a spin structure with a CE type in the a–b-plane but a fourfold periodicity along the c-axis [5, 6, 11]. Interestingly, when the system enters the antiferromagmetic phase (AFI(CE)), the CO pattern changes into a $\alpha\alpha\alpha\alpha$-type or $\alpha\beta\alpha\beta$-type [5, 11].

Compared with the A-site-disordered $R_{0.5}A_{0.5}MnO_3$ (A = Sr, Ca), $RBaMn_2O_6$ displays remarkable features:

(1) the CO transition at T_{CO} far above 300 K,
(2) a new stacking variation of the CE-type CO with a fourfold periodicity along the c-axis (4CE-CO),
(3) the absence of the lowering of T_{CO} or T_C in the phase boundary between FM and COI(CE),
(4) the presence of a structural transition at T_t above T_{CO} and
(5) the electronic phase segregation in the end member $LaBaMn_2O_6$.

The relatively high T_{CO} and the absence of a critical region between CO and FM states can be understood as the effect of the absence of the A-site randomness. The 4CE-CO could originate from the layer-type order of A-site cations. On the other hand, features (4) and (5) are closely related to the inherent structural frustration. Considering the tolerance factors, $f_1 = 1.2$ for $Ba^{2+}/Mn^{3.5+}$ and $f_2 = 0.8$ for $Y^{3+}/Mn^{3.5+}$ [14], for example, each MnO_2 layer in $YBaMn_2O_6$ should feel strain forces with opposite signs (or a structural frustration) from the adjacent YO and BaO layers. With this frustration, one cannot achieve an adequate compensation for this structural mismatch only from the tilting of the rigid MnO_6 octahedra. As a consequence, the shape of the MnO_6 octahedron deviates heavily from the ideal (regular) octahedron in the way shown in figure 2(c); the MnO_2 planar oxygen ions (O_{pl}) are displaced greatly from the ideal position $z = 0.25$ toward the RO layer, and the apical oxygen ions (O_{ap}) including the RO layer are shortened while those including the BaO layer are elongated.

The structural transition at T_t is observed in the third group with larger mismatch between RO and BaO lattices. The PM phase above T_t has a triclinic $P1$ symmetry with a $\sqrt{2}a_p \times \sqrt{2}b_p \times 2c_p$ unit cell, while the PM′ phase below T_t has a monoclinic $P2$ symmetry with a $\sqrt{2}a_p \times \sqrt{2}b_p \times 2c_p$ unit cell. The detailed structural analyses were done in $YBaMn_2O_6$ by neutron diffraction [6]. The lattice parameters reduced to the primitive perovskite cell are shown in figure 5 as a function of temperature. According to Glazer's notation [15–17], the octahedral tilting is approximately described as $a^-b^-c^-$ in the PM′ phases, while it is $a^0b^-c^-$ in the PM phase. In the ordinary solid solution of $R_{0.5}A_{0.5}MnO_3$, the MI transition to the CO state is always accompanied by a drastic first-order structural phase transition [1]. In $YBaMn_2O_6$, however, the metallic behaviour is still retained in the PM′ phase despite the drastic first-order structural phase transition at T_t, where the magnetic interactions abruptly change from ferromagnetic above T_t to antiferromagnetic below T_t, as derived from the susceptibility–temperature curve [3, 5, 6]. Added to this, considering the unusual structural transition at T_t from the low-temperature pseudo-tetragonal (monoclinic) to the high-temperature pseudo-orthorhombic (triclinic), a hidden parameter may play a role in compensating for the lattice entropy. We propose the ab-plane orbital ordering in the PM′ phase, in which not the $d_{3x^2-r^2}/d_{3y^2-r^2}$ orbitals (responsible for the insulating CE structure below T_{CO}) but the $d_{x^2-y^2}$ orbitals are occupied. Actually, this orbital ordering is compatible with the increase of $(a_p + b_p)/2$ and the decrease of c_p (see figure 5) would be induced so as to relax the peculiar lattice distortion arising from both the layered structure and octahedral tilting.

The last feature, the coexistence of the FM and AFI(CE) phases in $LaBaMn_2O_6$, is an unexpected phenomenon. A similar coexistence has been observed in $R_{1-x}A_xMnO_3$ so far and attributed to the A-site randomness or fluctuation of composition [18]. In the phase diagram of $R_{0.5}A_{0.5}MnO_3$, there exists a critical region where the FM and CO interactions compete with each other and therefore the transition from FM to AFI(CE) as a function of temperature, which is responsible for CMR, is observable. Since the present system does not have such randomness, the observed electronic phase segregation is an essential behaviour caused by

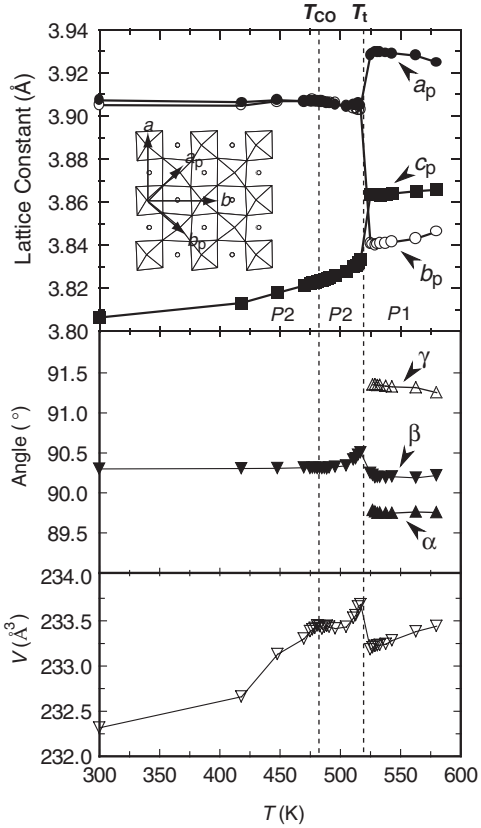

Figure 5. Temperature dependence of lattice parameters for $YBaMn_2O_6$. Lattice parameters are reduced to the simple perovskite cell.

the interplay among spin, charge, orbital and lattice degrees of freedom. If the ratio $r_{R^{3+}}/r_{Ba^{2+}}$ were an appropriate measure of the bandwidth as is the case of f for $R_{0.5}A_{0.5}MnO_3$, such a critical region would be located between $SmBaMn_2O_6$ and $NdBaMn_2O_6$, and an FM-to-AFI(CE) transition would be expected in $NdBaMn_2O_6$ adjacent to $SmBaMn_2O_6$. In reality, the ground state of $NdBaMn_2O_6$, however, is the A-type AFM and a fractional transition from FM to AFI(CE) is observed in $LaBaMn_2O_6$ far from $SmBaMn_2O_6$. This implies that $LaBaMn_2O_6$ might be located closer to the CO state and the bandwidth would become larger as $LaBaMn_2O_6 < PrBaMn_2O_6 < NdBaMn_2O_6$. Here it should be noticed again that $RBaMn_2O_6$ (R = La, Pr and Nd) has no tilt of MnO_6 octahedra. It is known that the tilt of MnO_6 octahedra in ordinary manganese perovskites occurs in order to fit the larger MnO_2 sublattice to the smaller AO sublattice ($f < 1$). No tilt of MnO_6 octahedra is expected to occur either when the MnO_2 lattice has almost the same size as the AO lattice ($f \approx 1$) or when the MnO_2 lattice is expanded by the AO lattice ($f > 1$). In $RBaMn_2O_6$ (R = La, Pr, Nd) with relatively larger R^{3+}, the expansion of the MnO_2 lattice by the much larger BaO lattice ($f = 1.071$) might overwhelm the contraction by the smaller RO lattice ($f = 0.982$ for LaO, $f = 0.964$ for PrO and $f = 0.950$ for NdO), in contrast to the case of $RBaMn_2O_6$ with R = Sm and later rare earth elements. Actually, the Mn–O_{pl} distance (∼1.96 Å) is elongated compared with that (1.91–1.94 Å) for the regular $Mn^{3.5+}O_6$. The increase of Mn–O_{pl} distance and the deviation

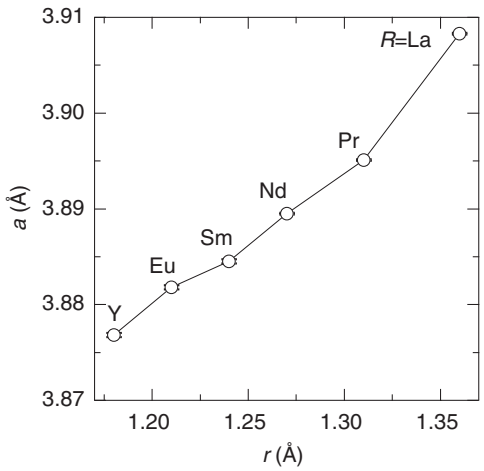

Figure 6. Lattice parameters of $R_{0.5}Ba_{0.5}MnO_3$ at room temperature as a function of the ionic radius of R^{3+}.

of the angle ∠Mn–O_{pl}–Mn from 180° would result in the decrease of bandwidth. In addition, the alternate stacking of RO and BaO layers would provide two-dimensional character in the structure, which would be preferable for the $d_{x^2-y^2}$ type orbital order (A-type AFM). These structural characteristics explain well the present results; no tilt structure stabilizes FM but the two-dimensional character in the structure leads to A-type AFM associated with $d_{x^2-y^2}$ type orbital order as the ground states of $NdBaMn_2O_6$ and $PrBaMn_2O_6$. The great elongation of Mn–O_{pl} distance in $LaBaMn_2O_6$ destabilizes FM to some extent as a result of the decrease of bandwidth and results in the fractional transition from FM to AFI(CE) (coexistence of FM and AFI(CE) phases as the ground state). The effect of Mn–O_{pl} distance on the bandwidth has never been seen or discussed in the ordinal perovskite manganese oxides, because they have finite tilt of MnO_6 octahedra, by which the bandwidth is dominantly controlled.

3.2. The A-site-disordered managanite, $R_{0.5}Ba_{0.5}MnO_3$

Lowering of both T_C and T_{CO} as observed in the critical region of $R_{0.5}A_{0.5}MnO_3$ is not recognized in the phase diagram of $RBaMn_2O_6$. The absence of such behaviour in $RBaMn_2O_6$ is partly due to the absence of the A-site randomness. In the critical region, the FM (AFM) and CO interactions compete with each other and are significantly affected by composition, coherent size of crystal, external field etc. The FM (AFM) and CO interactions are spatially distributed in $R_{0.5}A_{0.5}MnO_3$ with the A-site randomness. Such fluctuation of interactions enhances the criticality. On the other hand, it could be more definite which interaction becomes dominant in $RBaMn_2O_6$ without the A-site randomness. We may expect the critical competition of FM (AFM) and CO interactions in the disordered form. The disordered form with the same constituents is also important to study the A-site randomness effect at least qualitatively. We successfully synthesized the A-site-disordered managanite, $R_{0.5}Ba_{0.5}MnO_3$ [19]. The disordered form $R_{0.5}Ba_{0.5}MnO_3$ has a simple cubic cell. Figure 6 shows lattice parameters of $R_{0.5}Ba_{0.5}MnO_3$ at room temperature.

The results of electromagnetic properties are shown in figure 7 as a function of f. $R_{0.5}Ba_{0.5}MnO_3$ (R = La, Pr and Nd) with $f > 1$ is not mapped on the electronic phase diagram of ordinary $R_{0.5}A_{0.5}MnO_3$ with $f < 1$; nevertheless, we can expect FM as a dominant phase from the simple cubic structures. The ground state of $La_{0.5}Ba_{0.5}MnO_3$ is actually a pure

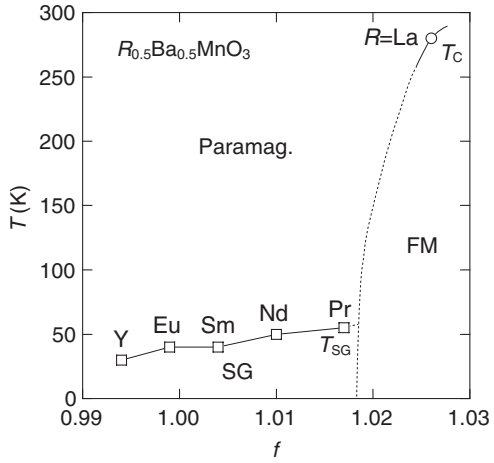

Figure 7. Phase diagram for $R_{0.5}Ba_{0.5}MnO_3$.

FM and the T_C decreases by 50 K compared with $T_C = 330$ K in $LaBaMn_2O_6$, agreeing with the previous report [8]. On the other hand, $Pr_{0.5}Ba_{0.5}MnO_3$ and $Nd_{0.5}Ba_{0.5}MnO_3$ show glassy behaviours below 50 K [19]. More typical spin-glass (SG) behaviours have been observed in $R_{0.5}Ba_{0.5}MnO_3$ with Sm^{3+} and smaller R^{3+}s [19]. The magnetic glassy state could be due to a disorder effect that hinders the long-range magnetic ordering and could occur as a result of the competition between randomly distributed ferromagnetic and antiferromagnetic interactions. Here it should be emphasized that the glassy state has never been observed in ordinary $R_{0.5}A_{0.5}MnO_3$ with A = Sr and Ca. Since the ionic radius of Ba^{2+} is much larger than that of Sr^{2+}, $R_{0.5}Ba_{0.5}MnO_3$ may include a spatial heterogeneity on a nanometre scale, which leads to the magnetic nonhomogeneous state. In the case of the largest La^{3+} among R^{3+}s only, a homogeneous solid solution with Ba^{2+} is formed in the A site of $La_{0.5}Ba_{0.5}MnO_3$ as in the case of $R_{0.5}A_{0.5}MnO_3$ and the long-range magnetic ordering (FM) is realized. Here, it should be noticed that the magnetic state of $R_{0.5}Ba_{0.5}MnO_3$ is significantly affected by the degree of the A-site disorder. The $R_{0.5}Ba_{0.5}MnO_3$ (R = La, Pr and Nd) prepared from annealing $RBaMn_2O_6$ has insufficient disorder of the A-site and shows the FM transition with monotonic decrease of T_C as La > Pr > Nd.

Very interestingly, a peculiar behaviour has been observed in $Pr_{0.5}Ba_{0.5}MnO_3$ at 2 K, as shown in figure 8. The resistivity decreases stepwise as the magnetic field increases, while the magnetization increases stepwise with a close relation to the resistivity behaviours. These behaviours are not reversible in the magnetic field. The stepwise behaviours in the magnetization and resistivity were observed up to 4.9 K but they vanished dramatically at 5.0 K. Similar behaviours were previously reported in $Pr_{0.5}Ca_{0.5}MnO_3$ doped with a few per cent of other cations such as Sc, Ga or Co on the Mn site and were explained by an impurity-induced disorder, with the coexistence of several short-range AFI(CE) phases and small FM regions [20, 21]. Our system has neither FM-to-AFI(CE) transition nor dopant, in contrast to $Pr_{0.5}Ca_{0.5}MnO_3$. This is the first observation of an ultrasharp magnetization and resistivity change in the nondoped system. A model based on an ordinal two-phase mixture cannot explain the behaviour. For instance, the AFI(CE) phase in coexistence with the FM phase is continuously converted to FM phase as observed in $LaBaMn_2O_6$ [7]. We have no explanation for such an ultrasharp magnetization and resistivity change at present. A detailed study is now in progress.

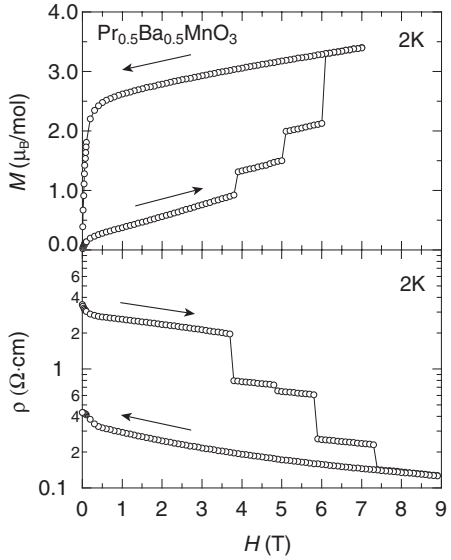

Figure 8. Magnetic field dependence of magnetization and resistivity at 2 K in $Pr_{0.5}Ba_{0.5}MnO_3$.

4. Summary

We have investigated the A-site-ordered/disordered manganite $RBaMn_2O_6$/$R_{0.5}Ba_{0.5}MnO_3$ (R = Y and rare earth elements). We have reviewed the structures and electromagnetic properties in this paper. The ordered form $RBaMn_2O_6$ displays remarkable features:

(1) the CO transition at T_{CO} far above 300 K,
(2) a new stacking variation of the CE-type CO with a fourfold periodicity along the *c*-axis (4CE-CO),
(3) the absence of the lowering of T_{CO} or T_C in the phase boundary between FM and COI(CE),
(4) the presence of structural transition possibly accompanied by $d_{x^2-y^2}$ orbital order at T_t above T_{CO} and
(5) the electronic phase segregation associated with the decrease of bandwidth caused by the elongation of Mn–O distance in the end member $LaBaMn_2O_6$.

The relatively high T_{CO} and the absence of a critical region between CO and FM states can be understood as the effect of the absence of the A-site randomness. The 4CE-CO could originate from the layer-type order of A-site cations, R and Ba. Features (4) and (5) are closely related to the structural characteristic that the MnO_2 square sublattice is sandwiched by two types of rock-salt layer, RO and BaO, with different lattice sizes. The large mismatch between RO and BaO lattices introduces a strong frustration to the MnO_2 sublattice and as a result the MnO_6 octahedron itself is heavily distorted. Such deformation must give a new perturbation to the competition of multiple degrees of freedom among charge, orbital, spin and lattice.

On the other hand, the disordered form $R_{0.5}Ba_{0.5}MnO_3$ has a primitive cubic perovskite cell. The electronic states characteristic of perovskite manganites are absent in $R_{0.5}Ba_{0.5}MnO_3$ and unexpectedly magnetic glassy states govern the electronic state of $R_{0.5}Ba_{0.5}MnO_3$. Since the ionic radius of Ba^{2+} is much larger than that of Sr^{2+} and also R^{3+}, $R_{0.5}Ba_{0.5}MnO_3$ may include a spatial heterogeneity on a nanometre scale, which leads to the magnetic nonhomogeneous state. The magnetic glassy state could be due to a disorder effect that hinders

the long-range magnetic ordering and could occur as a result of the competition between randomly distributed ferromagnetic and antiferromagnetic interactions. As remarkable phenomena in $R_{0.5}Ba_{0.5}MnO_3$, steplike ultrasharp magnetization and resistivity changes have been observed in $Pr_{0.5}Ba_{0.5}MnO_3$. Such behaviours could be closely related to a spatial heterogeneity of nanometre size.

Acknowledgments

The authors thank H Kageyama, M Ichihara, T Yamauchi, M Isobe, T Matsushita, Z Hiroi, H Fukuyama, K Ueda, H Yoshizawa and K Ohoyama for various experiments and valuable discussion. This work is partly supported by Grants-in-Aid for Scientific Research (no 407, no 758 and no 14340205) and for Creative Scientific Research (no 13NP0201) from the Ministry of Education, Culture, Sports, Science and Technology.

References

[1] See for reviews, Rao C N R and Raveau B 1998 *Colossal Magnetoresistance, Charge Ordering and Related Properties of Manganese Oxides* (Singapore: World Scientific)
[2] Mori S, Chen C H and Cheong S-W 1998 *Phys. Rev. Lett.* **81** 3972
[3] Nakajima T, Kageyama H and Ueda Y 2002 *J. Phys. Chem. Solids* **63** 913
[4] Nakajima T, Kageyama H, Yoshizawa H and Ueda Y 2002 *J. Phys. Soc. Japan* **71** 2843
[5] Kageyama H, Nakajima T, Ichihara M, Ueda Y, Yoshizawa H and Ohoyama K 2003 *J. Phys. Soc. Japan* **72** 241
[6] Nakajima T, Kageyama H, Ohoyama K, Yoshizawa H and Ueda Y 2004 *J. Solid State Chem.* **177** at press
[7] Nakajima T, Kageyama H, Ohoyama K, Yoshizawa H and Ueda Y 2003 *J. Phys. Soc. Japan* **72** 3237
[8] Millange F, Caignaert V, Domengés B, Raveau B and Suard E 1998 *Chem. Mater.* **10** 1974
[9] Trukhanov S V, Troyanchuk I O, Hervieu M, Szymczak H and Barner K 2002 *Phys. Rev.* B **66** 184424
[10] Uchida M, Akahoshi D, Kumai R, Tomioka Y, Arima T, Tokura Y and Matsui Y 2002 *J. Phys. Soc. Japan* **71** 2605
[11] Arima T, Akahoshi D, Oikawa K, Kamiyama T, Uchida M, Matsui Y and Tokura Y 2002 *Phys. Rev.* B **66** 140408
[12] Wada T *et al* 1989 *Phys. Rev.* B **39** 9126
Otzschi K *et al* 1994 *Physica* C **235–240** 839
[13] Akahoshi D and Ueda Y 1999 *J. Phys. Soc. Japan* **68** 763
Akahoshi D and Ueda Y 2001 *J. Solid State Chem.* **156** 355
[14] Shannon R D and Prewitt C T 1969 *Acta Crystallogr.* B **25** 925
[15] Glazer A M 1972 *Acta Crystallogr.* B **28** 3384
[16] Woodward P M 1997 *Acta Crystallogr.* B **53** 32
[17] Woodward P M 1997 *Acta Crystallogr.* B **53** 44
[18] Kawano H, Kajimoto R, Yoshizawa H, Tomioka Y, Kuwahara H and Tokura Y 1998 *Preprint* cond-mat/9808286
[19] Ueda Y and Nakajima T 2004 *J. Alloys Compounds* at press
[20] Hébert S, Hardy V, Maignan A, Mahendiran R, Hervieu M, Martin C and Raveau B 2002 *J. Solid State Chem.* **165** 6
[21] Mahendiran R, Maignan A, Hébert S, Martin C, Hervieu M, Raveau B, Mitchell J F and Schiffer P 2002 *Phys. Rev. Lett.* **89** 286602